szek and J. A. Mckee, *Tetrahedron Lett.*, **28**, 4511 (1987).
7. For a review of recent work, see (a) M. M. Midland, "*Asymmetric Synthesis*", J. D. Morrison, ed.: Academic Press: New York, 1983; Vol. 2, Chapter 2; (b) E. R. Grandbois, S. I. Howard, and J. D. Morrison, *ibid.*, Chapter 3; (c) H. Haubenstock, *Top. Stereochem.*, **14**, 231 (1983); (d) J. W. ApSimon and T. Lee Collier, *Tetrahedron*, **42**, 5157 (1986); For a comparative work, see: H. C. Brown, W. S. Park, B. T. Cho, and P. V. Ramachandran, *J. Org. Chem.*, **52**, 5406 (1987).
8. K. W. Whaley and T. R. Govindachari, *Org. Reactions.*, **6**, 74 (1951).
9. K. Yamada, M. Takeda, and T. Iwakuma, *J. Chem. Soc. Perkin Trans. 1*, 265 (1983).
10. B. T. Cho and C. K. Han, *Bull. Korean Chem. Soc.*, **11**, 81 (1990).
11. K glucoride: Potassium 9-O-(1,2; 5,6-di-*O*-isopropylidene-α-D-glucofuranosyl)-9-boratobicyclo-[3.3.1.]nonane: H. C. Brown, B. T. Cho, and W. S. Park, *J. Org. Chem.*, **53**, 1231 (1988).
12. BH_3-AMDPB (2 : 1): AMDPB=(S)-(−)-2-amino-1,1-diphenylbutan-1-ol: S. Itsuno, M. Nakano, K. Miyazaki, H. Matsuda, K. Ito, A. Hirao, and S. Nakahama, *J. Chem. Soc. Perkin Trans. 1*, 2039 (1985). In this paper, a defined structure of the reagent was not reported, but the structure of **6** became apparent after Corey's work: E. J. Corey, R. K. Bakshi, and S. Shibata, *J. Am. Chem. Soc.*, **109**, 5551 (1987).
13. $LiAlH_4$-Darvon alcohol (1 : 1): Darvon alcohol=[2S, 3R]-(+)-4-(dimethylamino)-3-methyl-1,2-diphenyl-2-butanol: S. Yamaguchi, and H. S. Mosher, *J. Org. Chem.*, **38**, 1870 (1973).
14. R. O. Hutchins, A. Abdel-Magid, Y. P. Stercho, and A. Wambsgans, *J. Org. Chem.*, **52**, 704 (1987).
15. S. Teitel, J. O'Brien, W. Pool, and A. Brossi, *J. Med. Chem.*, **17**, 134 (1974).
16. E. Yamato, M. Hirakura, and S. Sugasawa, *Tetrahedron, Suppl.* 8, part 1, 129 (1966).
17. *Beilstein* E 3/4, **21**, 2612.
18. *Beilstein* E 3/4, **21**, 2704.
19. A. Brossi and S. Teitel, *Helv. Chim. Acta*, **54**, 1564 (1972).
20. S. Teitel, J. O'Brien, and A. Brossi, *J. Med. Chem.*, **15**, 845 (1972).
21. L. Gottlieb and A. I. Meyers, *J. Org. Chem.*, **55**, 5659 (1990).
22. *Organic Synth., Col.* **6**, 3.
23. *Beilstein* E **4**, 2735.
24. K. Leader, B. Lünnig, annd E. Ruusa, *Acta Chem. Scand.*, **23**, 244 (1969).
25. J. Knabe and A. Schepers, *Arch. Pharm.*, **295**, 31 (1962).
26. *Beilstein* E4, 2735.
27. H. C. Brown, G. W. Kramer, A. B. Levy, and M. M. Midland, "*Organic Synthesis via Boranes*", Wiley-Interscience; New York, 1975.

Probe Diffusion in Polymer Solutions by Forced Rayleigh Scattering

Jaeyung Lee, Taiho Park, Jungmoon Sung, Sangwook Park, and Taihyun Chang*

Department of Chemistry, POSTECH, P.O.Box 125, Pohang 790-600
Division of Organic Materials, RIST, Pohang 790-600. *Received June 24, 1991*

Methyl red diffusion in polymer solutions was studied by a transient holographic method, forced Rayleigh scattering. In semi-dilute solutions of a polystyrene, where no specific interaction with the probe exists, we found within experimental uncertainty that the retardation of diffusion rate of methyl red is independent of the solvents used. This indicates that the hydrodynamic interaction in polymer coils is not affected by the nature of solvents enough to exhibit a detectable change in the diffusion rate of the probe. On the other hand, a substantial reduction of diffusion rate was observed in poly (methyl methacrylate) solutions in toluene. Together with the similar observation reported with poly (vinyl acetate), it is confirmed that hydrogen bond between the probe and the polymer is responsible for the retarded diffusion. The decay-growth-decay profile found in this system reveals a finite difference in diffusion coefficients of *cis* and *trans* isomer of methyl red. We estimate the difference and suggest that the *cis* isomer interacts with the polymer more strongly than the *trans* isomer.

Introduction

The study of probe diffusion in polymer solutions and polymer gels provides basic knowledges regarding the molecular sieving process which constitutes the basis of many applications in material separation process such as gel filtration, separation membrane etc. The diffusion of probes through mesh like structure of polymer chains are known to be influenced by the size of diffusant and polymer concentration for a given polymer solution system. It is generally believed that a stretched exponential form can describe the diffusion behavior,

*To whom correspondence should be addressed.

$$D/D_O = \exp(-R\,c^{\nu}) \quad (1)$$

where R the size parameter of the probe, c the concentration of polymers and v is the characteristic exponent of the system.[1-3]. According to the scaling theory,[4,5] the exponent, v is related to the hydrodynamic screening length of polymer matrix and is in the range of 1/2 to 1 depending on the solvent quality.[6] It was confirmed that Eq. (1) works reasonably well for a good solvent system.[1] However, a systematic study with varying solvent quality is yet to be attempted and deviations from above prediction have been reported.[2,7] Therefore it cannot be said that Eq. (1) has been fully tested. Furthermore, when a specific interaction between the probe and the polymer backbone exists, one may not expect that Eq. (1) still holds. For an example, it was reported some years ago that the diffusion rate of methyl red (MR) was much lower in toluene solution of poly (vinyl acetate) (PVAc) than that of polystyrene (PS).[8] The hydrogen bonding between MR and PVAc was suggested to be responsible for the retarded diffusion.

In this study, we measured the MR diffusion in semidilute polystyrene and poly (methyl methacrylate) (PMMA) solutions to examine the forementioned problems. We used forced Rayleigh scattering (FRS) which is an optical technique to measure tracer diffusion suitable for this purpose.[1,2,8-11] The technique requires a photoresponsive probe which changes own optical properties upon absorption of writing beams. Azobenzene derivatives such as methyl red, which have been widely used for FRS, is known to undergo *trans* to *cis* photoisomerization upon absorption of the light which causes n-π^* transition of the lone pair electrons.[12,13] Crossing two coherent laser beams (writing beam) as the specimen creates a periodic optical fringe pattern which gives rise to a periodic concentration profile of optically shifted state of the probe. The concentration fringe pattern in turn acts as an optical grating to diffract the second (reading) beam. In order to induce the diffraction of the reading beam, the shifted state should possess different optical properties from unshifted state of the probe either in absorptivity or in refractive index which are called as amplitude and phase grating, respectively.[14-16] Azobenzene derivatives, having a negligible absorptivity at the typical reading beam wavelength of 632.8 nm, should form almost a pure phase grating. Diffracted reading beam decays with time due to the diffusion as well as the spontaneous thermal reconversion of the shifted state of the probe and one can determine the diffusion coefficient and the shifted state life-time from an appropriate analysis of decay profile.

Experimental

Materials. Solvents used in this study, toluene, CCl_4, tetrahydrofuran (THF), 2-butanone and ethyl acetate, were all reagent grades (Aldrich) and further purified by fractional distillation after drying with proper agents. Methyl red was used as received from Aldrich. Probe dye concentration was 0.1 to 0.5 mg/m*l* and it was confirmed that the measured diffusion coefficients do not show any concentration dependence at this concentration range.

Used polystyrene was prepared in this laboratory by anionic polymerization. Its weight average molecular weight and

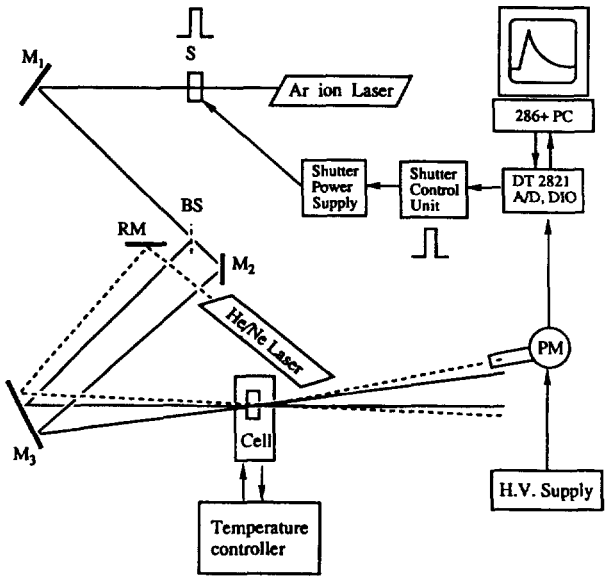

Figure 1. Schematic Diagram of FRS apparatus. S: electronic shutter, BS: beam splitter, M_1, M_2, M_3, RM: mirrors, PM: photomultiplier tube.

M_w/M_n were determined by gel permeation chromatography as 660 K (dalton) and 1.09, respectively. A poly (vinyl acetate) and two poly (methyl methacrylate) were obtained from Aldrich and their detailed molecular characteristics were not provided. GPC analysis with repect to polystyrene standards yields M_w and M_w/M_n of 85.6 K, 1.13 for PVAc and 736 K, 6.75 for high molecular weight PMMA, 75.5 K, 1.98 for medium molecular weight PMMA, respectively.

Solutions of respective polymers were prepared by gravimetrically and converted to volume fractions from the density of the materials. Prepared polymer solutions with methyl red were filtered through 0.45 μm pore PTFE membrane filters (Gelman) directly to spectroscopic cuvettes for FRS measurements.

Methods. Forced Rayleigh scattering instrument was built in this laboratory and its schematic diagram is shown in Figure 1. The 488 nm line of an Ar ion laser (Coherent, Model 90-3) and an electronic shutter (Uniblitz, LS2) is used to generate a short pulse of the writing beams which cross at the sample cell. A He/Ne laser (Melles Griot, 5 mW) provides the 632.8 nm wavelength reading beam which continuously illuminates the spot where writing beams cross each other. Intensity of the He/Ne laser was controlled by inserting neutral density filters, if necessary. The diffracted light was detected by a photomultiplier tube (Hamamatsu, R-928). Triggering of the shutter and the subsequent data acquisition are carried out by an IBM AT compatible personal computer through an interface board (Data Translation, DT2821-F-8DI) with a maximum throughput rate of 150 kHz. Spectroscopic cuvettes (1, 2 or 5 mm pathlength) were used as sample cells and the temperature of the cell was controlled at 25.0± 0.1℃. Although we found no pathlength dependence of diffusion coefficients under our experimental condition, a longer pathlength cell was preferred since a similar quality of signal can be achieved at a lower probe concentration.

Decay profile of diffracted intensity showing single ex-

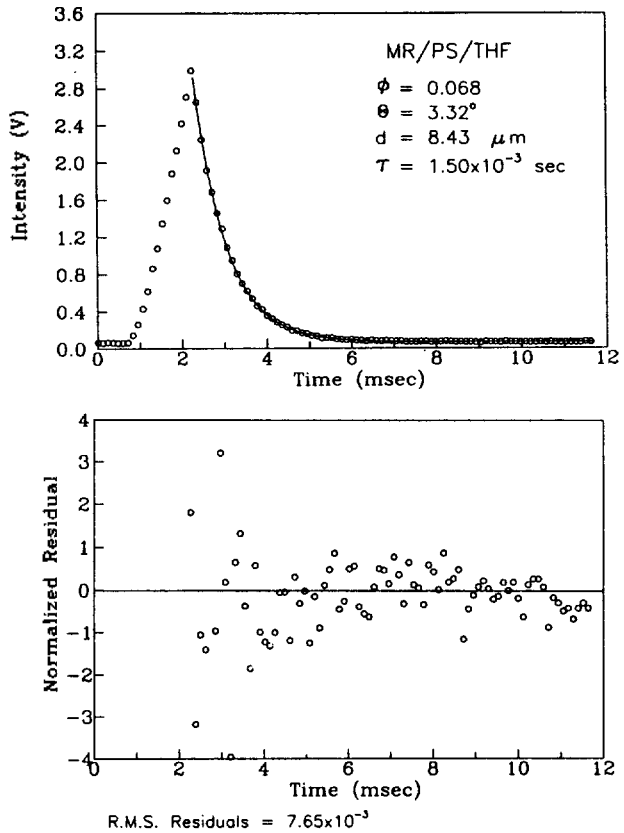

Figure 2. A typical FRS profile of methyl red in polystyrene /THF solution. In upper plot, circles represent the experimental result and the solid line is the best fit result according to Eq. (2). Random residuals from fitting shown in the lower plot together with the small value of root-mean-square residuals illustrate the quality of the fit. Experimental conditions, volume fraction, ϕ, crossing angle, θ, and grating spacing, d are shown in the plot as well as the determined decay time constant, τ.

ponential form was analyzed by fitting to the model function[17]

$$I_d(t)=[A\ \exp(-t/\tau)+B_{coh}]^2+B_{inc} \quad (2)$$

where A the amplitude of the diffracted optical field, τ the decay time constant of the concentration grating, B_{coh} the coherent background, and B_{inc} is the incoherent background. Decay time constants were determined at a number of fringe spacing, $d=\lambda/[2\sin(\theta/2)]$ where θ is the crossing angle of the writing beams. Tracer diffusion coefficient was obtained from the slope of the $1/\tau$ *vs.* $4\pi^2/d^2$ plot according to the relation,[17]

$$1/\tau=1/\tau_{life}+4\pi^2D/d^2 \quad (3)$$

where τ_{life} is the spontaneous thermal reconversion life-time for the shifted state. When decay-growth-decay type signal (see next section) was observed, it was analyzed by fitting to[18]

$$I_d(t)=[A_1\ \exp(-t/\tau_1)-A_2\ \exp(-t/\tau_2)]^2+B \quad (4)$$

where τ_1 and τ_2 are decay time constants of two complementary gratings, B the baseline, and A_1 and A_2 represent the amplitude of optical fields diffracted from individual complementary gratings. Here, we neglected the coherent background since it was found to yield more reproducible fitting results and its contribution was small for optically clear samples. We found that thus determined τ_1 and τ_2 fluctuate depending on initial guess of the parameters for regression analysis, about ± 15% in the worst case, but their mean values are quite reproducible as reported by others.[8,18] Therefore, we can not obtain the individual diffusion coefficient with accuracy unless other parameters are known, however, the use of mean values can be justified since they are reproducible and the diffusion coefficients of *cis* and *trans* azobenzene do not differ much.[19]

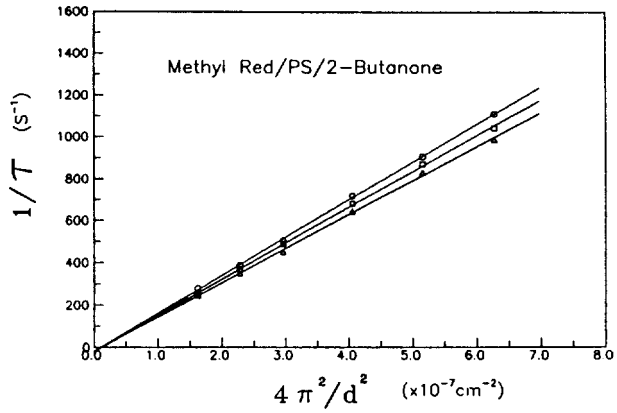

Figure 3. Grating spacing dependence of decay time constants. Diffusion coefficients are extracted from the slope of the least square fit line according to Eq. (3). Different symbols represent the polystyrene volume fraction in 2-butanone solution. ○: 0.013, □: 0.024, △: 0.035.

Results and Discussion

In Figure 2 is shown a typical FRS signal measured in polystyrene solution. The solid line in the plot represents the fitting result according to Eq. (2). It is evident from the residual plot that the single exponential model function fits the experimental data well. In most of the cases, the contribution of coherent baseline was found to be very small which justifies our neglect of B_{coh} in Eq. (4) for the decay-growth-decay profile to be illustrated later. Since there was a report for the possible association of the probe dye upon photoexcitation,[20] we examined the decay time constant at various laser intensity. At very high laser intensity, we observed an anomalous rising profile of FRS signal, but the decay time constant remains practically unchanged.

Decay time constant of diffracted optical field was measured at a number of different grating spacings and the tracer diffusion coefficient was determined from the plot according to Eq. (3) as shown in Figure 3. In the plot, the data taken at three different polystyrene concentrations were shown. It is clearly seen that the slope representing the diffusion coefficient of MR decreases with polymer concentration. Also the intercepts hit the origin within experimental uncertainty, which means that the life-time of the *cis* state of methyl red is much longer than the decay time constant of concentration grating by diffusion. In Figure 4, the diffusion coefficients of methyl red are plotted against the volume fraction of the polymer, ϕ in 5 different solvents. The diffusion coefficients, D are normalized by the diffusion coefficient measu-

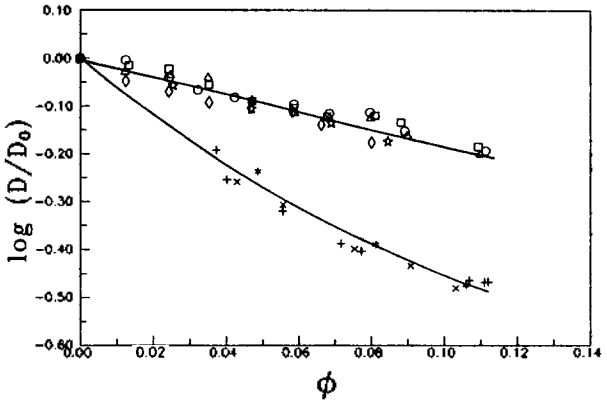

Figure 4. Diffusion coefficients of methyl red, normalized by the diffusion coefficient in pure solvent, D/D_o are plotted as a function of polymer volume fraction. The group of symbols consisting the upper line are from polystyrene solution in 5 different solvents. ○: THF, □: toluene, △: CCl_4, ◇: 2-butanone, ☆: ethyl acetate. Other symbols are from toluene solutions of PMMA and PVAc. +: PVAc, ×: medium mol. wt. PMMA, ✳: high mol. wt. PMMA. Solid lines are drawn for visual aid.

red in pure solvents, D_o. Although the solvent property of these 5 solvents varies much, all data points form a single line within experimental uncertainty (typically ~10% in 95% confidence limit from the least square analysis such as shown in Figure 3) regardless of the solvent used. Therefore there is no strong solvent effect enough to be isolated under this experimental condition. However, it is premature to claim the absence of the solvent dependence with this experiment alone since the dependence of diffusion coefficient on solvent quality[5,6] may be too weak to be detected with precision. In fact, the analysis to extract v in Eq. (1) was not satisfactory because the variation of the diffusion coefficient is not much larger than experimental uncertainty. According to Eq. (1), the increase of probe size should enhance the variation of D/D_o, and one can get a better insight with a given experimental precision. Such experiment is in progress with larger probes, polystyrenes chains labeled with an azo dye.[1]

On the other hand, the FRS signal from a PMMA/toluene solution shows a non-single exponential decay as displayed in Figure 5. A similar decay-growth-decay profiles were observed in PVAc/toluene system as reported before.[8] The solid line is the best fit result according to Eq. (4). As can be seen in the residual plot, the quality of the fit is not as good as the case of single exponential decay (Figure 2). Therefore, we could not obtain two independent diffusion coefficients with accuracy, but only report mean values as mentioned previously. The mean decay constants exhibit an excellent d^2 dependence as in Figure 6 from which the diffusion coefficients are extracted. We plotted all the diffusion coefficients thus determined in Figure 4. Clearly the diffusion of MR in PVAc or PMMA/toluene solution is greatly retarded by the presence of the polymers. The similar retardation observed in PVAc and PMMA, which have very close functional group structures, convincingly supports the view that the slower diffusion in PVAc/toluene solution arises from hydrogen bond formation between carboxylic hydrogen in MR and the carbonyl group in the polymers. It is interesting to note a similar extent of retardation for the polymers having different structure and molecular weights. Although the insensitiveness of probe diffusion coefficients to the matrix molecular weight is generally accepted for the cases without specific interaction,[17,21] the same can not be said for this case. The similar diffusion coefficients found in PMMA and PVAc solutions indicate that the probe/poly-

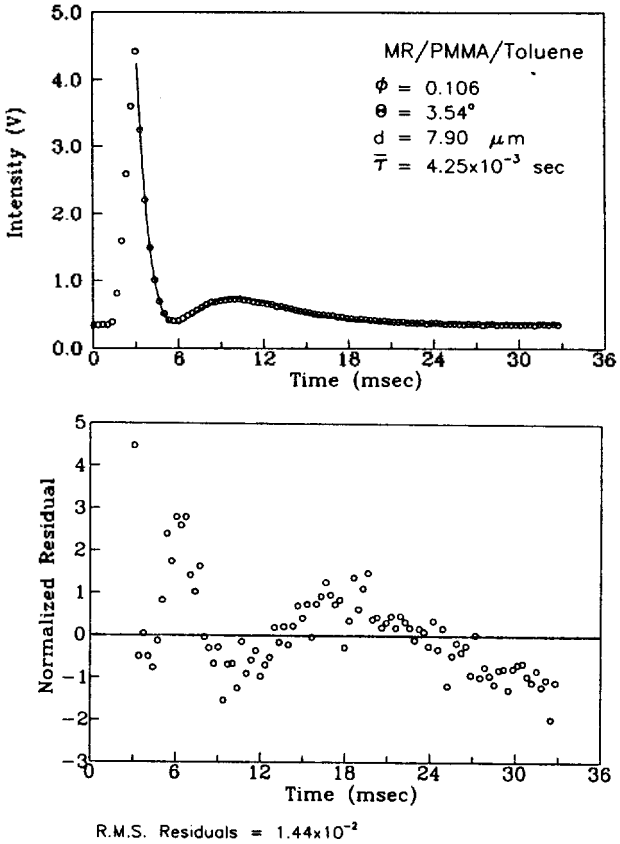

Figure 5. An FRS profile of methyl red in PMMA/toluene solution and fit result according to Eq. (4).

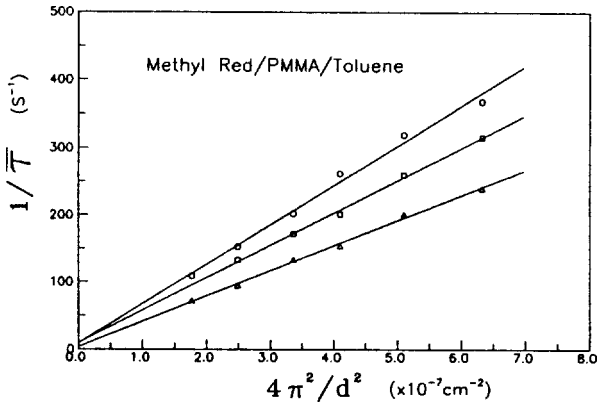

Figure 6. Grating spacing dependence of mean decay time constants. Diffusion coefficients are extracted from the slope of the least square fit line according to Eq. (3). Different symbols represent the PMMA volume fraction in toluene solution. ○: 0.049, □: 0.081, △: 0.106.

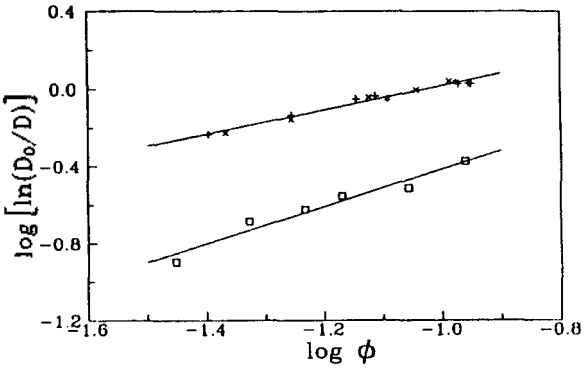

Figure 7. ln (D_o/D) plotted against polymer volume fraction, ϕ, in double logarithmic scale. Symbols are experimental results in toluene solutions and the exponent ν is obtained by least square analysis drawn as solid lines. □: polystyrene, +: PVAc, ×: medium mol. wt. PMMA, *: high mol. wt. PMMA.

mer interaction is quite similar for PVAc and PMMA, which seems reasonable considering similar structure of two polymers. In Figure 7 is shown a plot to extract the exponent ν in Eq. (1). Taking a double logarithm for the ordinate demands a high precision of data to render the analysis significant. Our data are somewhat scattered but show a good linearity enough to yield a slope, $\nu=0.65\pm0.07$ in 95% confidence limit. Therefore, it appears that the stretched exonential form of Eq. (1) still reasonably describes the diffusion process in a system with specific interaction such as hydrogen bonding. For comparison, we showed the results from the polystyrene/toluene solution in the same figure. The exponent found in polystyrene/toluene solution is 0.98 ± 0.31.

The observed decay-growth-decay profile needs an additional explanation. This behavior is generally accounted for as a result of mutual destructive interference between the optical fields diffracted from two complementary gratings.[18,22,23] Making a sinusoidal pattern of the shifted state of a probe (*cis* state of methyl red, in this case) during the writing process depletes the unshifted state at the same time, generating a complementary pattern of the unshifted state. These two concentration fringes are physically 180° out of phase each other. Since each concentration fringe can act as a diffraction grating of the reading beam so that the observed signal is the difference of these two diffracted optical fields as represented by Eq. (4). If the decay time constants of two complementary gratings, τ_1 and τ_2 are not much different, Eq. (4) is reduced to Eq. (2). Otherwise, a deviation from a single exponential form takes place. Also the relative difference of A_1 and A_2 affects the signal shape, which depends on the relative absorptivity and refractive index of the dye to those of background. For an unslanted grating, the coupled-wave theory gives the diffracted optical wave E^o_d from a weak diffraction grating.[14,16,22]

$$E^o_d \propto [-i(\Delta n)+(\Delta k)] \tag{5}$$

where Δn and Δk are the gratings peak-null differences in real and imaginary part of complex refractive index, respectively. The diffraction efficiency is given by $|E^o_d|^2$, thus

$$I_d/I_o \propto [(\Delta n)^2+(\Delta k)^2] \tag{6}$$

where I_o is the incident light intensity. Eq. (5) shows that a pure absorption grating ($\Delta n=0$) introduces no phase shift while light diffracted from a pure phase grating ($\Delta k=0$) is shifted by $-\pi/2$. For an arbitrary grating in the weak grating limit, the phase shift is given by

$$\varphi=\sin^{-1}|-\Delta n/[(\Delta n)^2+(\Delta k)^2]^{1/2}| \tag{7}$$

This phase information is lost in the detection of diffracted light from a single grating by a square-law detector such a photomultiplier. However, the phase difference plays a role when the complementary grating is in effect. Therefore Eq. (4) should be written considering this effect that

$$\begin{aligned} I_d(t) &= |E_d(t)\cdot E_d^*(t)| \\ &= [A_1\exp(-t/\tau_1)+A_2\exp(-t/\tau_2)\exp(i\ \Delta\varphi)]\times \\ &\quad [A_1\exp(-t/\tau_1)+A_2\exp(-t/\tau_2)\exp(-i\ \Delta\varphi)]+B \end{aligned} \tag{8}$$

where $\Delta\varphi$ is the phase difference between the diffracted waves from two complementary gratings, *i.e.*, $\Delta\varphi=\pi+(\varphi_1-\varphi_2)$. For most of azobenzene derivatives, absorptivity of the dye is very small at the reading beam wavelength of 632.8 nm. Therefore the diffracted intensity is mainly the contribution of phase grating, *i.e.*, $\Delta\varphi\simeq\pi$, which reduces Eq. (8) to Eq. (4) justifying our analysis scheme. We reported the problems associated with such complementary gratings through a simulation study.[24]

Returning to our experimental system, the double exponential decays observed in PVAc or PMMA/toluene solutions indicate that two decay constants, τ_1 and τ_2 differ more in these solutions than PS solutions. Although we cannot elucidate this phenomenon at the moment without having detailed knowledge about their optical properties on hand, it is possible to give a rough estimate for the difference of τ_{trans} (τ_1) and τ_{cis} (τ_2) assuming the refractive index of methyl red is the same as that of stilbene ($n_{trans}=1.626$ and $n_{cis}=1.613$).[25] This assumption is certainly a rough but an acceptable approximation since stilbene and azobenzene are isoelectronic. In fact, the refractive index of *trans* azobenzene is 1.627, which is very close to that of stilbene. Isolation of pure *cis* isomer of azobenzene derivatives is only reported for azobenzene. Nonetheless, its refractive index is not available to the best of our knowledge. For other derivatives like methyl red, pure *cis* form has not been isolated due to their short lifetime. From these refractive indices together with that of toluene (1.496), we obtained $A_1:A_2=(n_{trans}-n_{toluene}):(n_{cis}-n_{toluene})=10:9$. We carried out a nonlinear regression fitting for the same data shown in Figure 5 under the constraint of fixed A_2/A_1 at 0.9. The fit quality was similar to that in Figure 5 and we obtained $\tau_1=3.8$ ms, $\tau_2=4.7$ ms. The difference in decay time constants indicates that the diffusion rate of *cis* isomer is lower than *trans* isomer by about 20%, which in turn suggests that *cis* isomer interacts with PMMA or PVAc more strongly than *trans* isomer. Although the quantitative amount of the difference is subject to the values of refractive indices of methyl red and thus questionable, the trend should stand firm. *Cis* form of azobenzene derivative is known to have two phenyl groups twisted by steric effect while the *trans* form has a coplanar structure.[12,13] Therefore, the breakage of conjugated π electron system by *trans* to *cis* isomerization probably alters the hydrogen bonding capability so that *cis* isomer can form a more strong hydrogen bonding with the polymers. Although fur-

ther studies are necessary to elucidate the observed difference, this analysis demonstrates one of the remarkable feature of FRS that one can measure a *differential* diffusion coefficient provided A_1 and A_2 are known. Indeed, FRS is a very sensitive and versatile technique to measure tracer diffusion coefficient, but it is indispensable for an accurate interpretation of FRS data to know about the optical properties of the probe in the system of interest. It can not be said, however, that appropriate care has been paid so far.

Acknowledgement. This work was financially supported in part by grants from the Ministry of Education and from the Korean Science and Engineering Foundation.

References

1. T. Chang, H. Kim, and H. Yu, *Macromolecules*, **20**, 2629 (1987) and references therein.
2. I. H. Park, C. S. Johnson, Jr., and D. A. Gabriel, *Macromolecules*, **23**, 1548 (1990) and references therein.
3. R. Furukawa, J. L. Arauz-Lara, and B. R. Ware, *Macromolecules*, **24**, 599 (1991) and references therein.
4. P.-G. de Gennes, *Scaling Concepts in Polymer Physics*, Cornell Univ. Press, Ithaca (1979).
5. D. Langevin and F. Rondenlez, *Polymer*, **19**, 875 (1978).
6. R. I. Cukier, *Macromolecules*, **17**, 252 (1984).
7. G. S. Ullman, K. Ullman, R. M. Linder, and G. D. Phillis, *J. Phys. Chem.*, **89**, 652 (1985).
8. J. A. Lee and T. P. Lodge, *J. Phys. Chem.*, **91**, 5546 (1987).
9. H. Hervet, W. Urbach, and F. Rondelez, *J. Chem. Phys.*, **68**, 2725 (1978).
10. J. A. Wesson, H. Takezoe, H. Yu, and S. P. Chen, *J. Appl. Phys.*, **53**, 6513 (1982).
11. H. Sillescu, C. H. Wang, and J. Coutandin, *Macromolecules*, **18**, 587 (1985).
12. D. L. Ross and J. Blanc in *Photochromism*, G. H. Brown ed., Wiley, New York, Chapter 5 (1972).
13. A. V. El'tsov, *Organic photochromes*, Plenum, New York p. 112 (1990)
14. H. Kogelnik, *Bell Syst. Tech. J.*, **48**, 2909 (1969).
15. A. von Jena and H. E. Lessing, *Opt. Quantum Electron.*, **11**, 419 (1979).
16. K. A. Nelson, R. Casalegno, R. J. Dwayne Miller and M. D. Fayer, *J. Chem. Phys.*, **77**, 1144 (1982).
17. H. Kim, T. Chang, J. M. Yohanan, L. Wang, and H. Yu, *Macromolecules*, **19**, 2737 (1986).
18. W. J. Huang, T. S. Frick, M. R. Landry, J. A. Lee, T. P. Lodge, and M. Tirrell, *AICHE J.*, **33**, 573 (1987).
19. L. S. Lever, M. S. Bradley, and C. S. Johnson, Jr., *J. Mag. Res.*, **68**, 335 (1986).
20. W. Urbach, H. Hervet, and F. Rondelez, *J. Chem. Phys.*, **83**, 1877 (1985).
21. M. R. Landry, Q. Gu, and H. Yu, *Macromolecules*, **21**, 1158 (1988).
22. C. S. Johnson, Jr., *J. Opt. Soc. Am. B*, **2**, 317 (1985).
23. H. Kim, Ph. D. Dissertation, University of Wisconsin-Madison (1987).
24. S. Park, J. Sung, H. Kim, and T. Chang, *J. Phys. Chem.*, in press.
25. R. C. Weast ed., *Handbook of Chemistry and Physics, 70th Ed.*, CRC Press (1989).

A Theoretical Study of CO Molecules on Metal Surfaces: Coverage Dependent Properties

Sang -H. Park and Hojing Kim*

Department of Chemistry, Seoul National University, Seoul 151-742. *Received June 26, 1991*

The CO molecules adsorbed on Ni(111) surface is studied in the cluster approximation employing EH method with self-consistent charge iteration. The effect of CO coverage is simulated by allowing the variation of valence state ionization potentials of each Ni atom in model cluster according to the self-consistent charge iteration method. The CO coverage dependent C-O stretching frequency shift, adsorption site conversion, and metal work function change are attributed to the charge transfer between metal surface and adsorbate. For CO/Ni(111) system, net charge transfer from Ni surface to chemisorbed CO molecules makes surface Ni atoms be more positive with increasing coverage, and lowers Ni surface valence band. This leads to a weaker interaction between metal surface valence band and Co $2\pi^*$ MO, less charge transfer to a single CO molecule, and the bule shift of C-O stretching frequency. Further increase of coverage induces the conversion of 3-fold site CO to lower coordination site CO as well as the blue shift of C-O stretching frequency. This whole process is accompanied by the continuous increase of metal work function.

Introduction

One of the most extensively studied adsorbates is carbon monoxide. Its interaction with metal surfaces has constituted the model systems for molecular chemisorption for many years. When a CO molecule is adsorbed on a metal surface, the vibrational frequency ω_{CO} of the intramolecular stretching mode exhibits substantial downward shift from its gas phase value at 2143 cm^{-1}. It has been widely accepted that the 5σ orbital of the CO molecule is primarily responsible for